Advanced Laser System with Stable Reflection Using Brewster Pick-Off

Jean-Charles Cotteverte¹ and Alan Cox

¹JCC-consulting (jcc-consulting.co.uk), Greater Manchester, UK

February 2025

Abstract

Optical systems often suffer from performance degradation due to contamination. The vertically tilted Brewster pick-off, as described in US Patent 2016033775 A1, offers a novel approach to maintain stable reflection properties under varying environmental conditions. The system leverages a partial reflector with a specific orientation relative to the laser beam's polarization plane, ensuring that the reflected fraction of the laser beam remains invariant to changes in temperature and contamination layer thickness. By utilizing Brewster's angle and optimizing the polarization angle, the system achieves a reflected fraction that is both stable and minimally affected by environmental factors. This innovation is particularly beneficial for applications requiring precise control and measurement of laser beam properties. This white paper expands on the fundamental principles of the vertically tilted Brewster pick-off and highlights its effectiveness in mitigating contamination effects and details the theoretical foundation and practical implications of this technology. The effect of degree of polarization is also considered.

Introduction

The stability of laser beam reflection is crucial in various scientific and industrial applications. Traditional laser systems often face challenges related to environmental factors such as temperature variations and contamination-mainly caused by dust and airborne molecules—, which can alter the reflective properties of optical components. This white paper introduces a novel laser system that addresses these challenges by employing a partial reflector with a strategically oriented partially reflective surface. The system ensures that the fraction of the laser beam reflected for measurement or feedback control remains consistent, thereby enhancing the reliability and accuracy of laser-based applications. This paper builds upon the core concepts of the patented approach and explores its extended benefits. In a first part, the theoretical foundation will be developed. Then, further considerations will be addressed, especially the effect of the degree of polarisation (DOP).

Theoretical Foundation

The core principle [1] behind the stability of the reflected fraction lies in the use of Brewster's angle and the manipulation of the polarization angle. Brewster's angle is the angle of incidence at which light with a particular polarization is perfectly transmitted through a transparent dielectric surface, with no reflection. Fig. 1 shows this with the reflectivity for s-pol and p-pol, calculated from Fresnel's formulas [2].

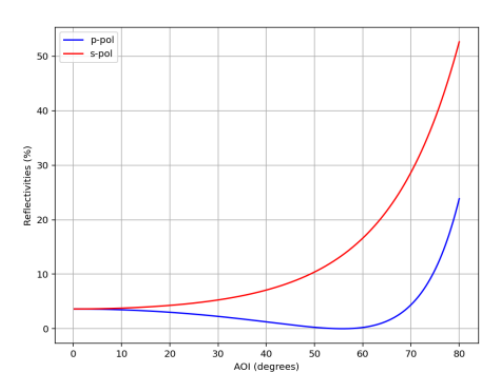


Fig. 1: Fresnel's curves for $n_{sub}=1.47$ (index of fused silica at 532 nm), in air $(n_0=1)$, for both polarisations, p-pol and s-pol. Here, Brewster's angle is 55.8 °.

We focus on the reflectivities around Brewster's angle, which are shown in Fig. 2. The curves are calculated for 3 similar refractive indices: $n_{sub} = 1.47$, $n_{sub} = 1.47 + 0.03$, $n_{sub} = 1.47 - 0.03$.

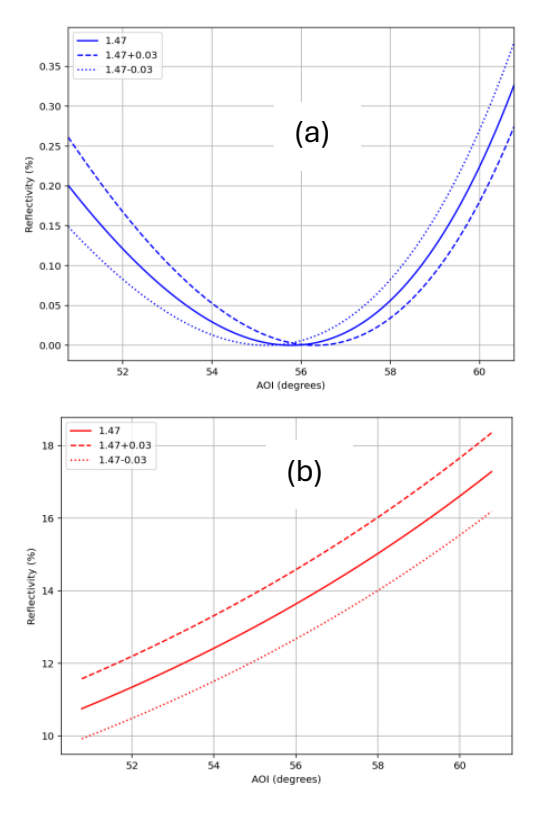


Fig. 2: Fresnel's curves zoomed around Brewster's angle, for $n_{sub}=1.47$ (index of fused silica at 532 nm), in air $n_0=1$, and also for $n_{sub}=1.47+0.03$ and $n_{sub}=1.47-0.03$ for both polarisations, p-pol (a) and s-pol (b).

One can see that for angles of incidence (AOIs) slightly above Brewster's angle, the change in reflectivity for both polarisation is opposite, so there should be a sweet spot where they might be evenly balanced if the polarization angle is purposely adjusted. Indeed, by orienting the partially reflective surface at an angle slightly greater than Brewster's angle and adjusting the polarization angle, the system might balance the p-polarized and s-polarized components of the laser beam, even if the reflectivities are significantly different. In the following, we will calculate this more specifically.

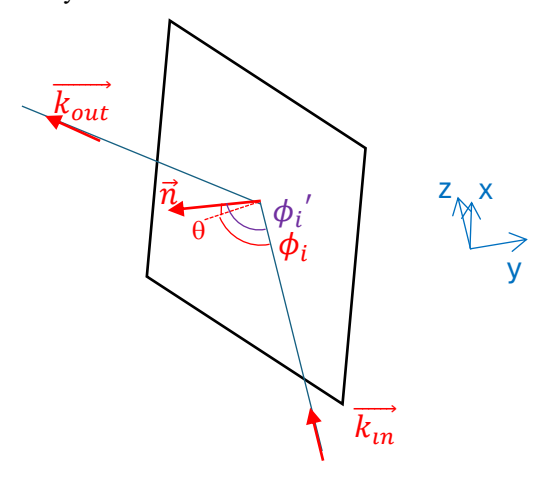


Fig. 3: Optical scheme of the system.

The optical scheme is shown in Fig. 3, for an input beam symbolized by $\overrightarrow{k_{in}}$, a horizontal angle ϕ_i , and a tilt angle θ . The normal vector of the surface is \overrightarrow{n} . The angle of incidence (AOI) is then ϕ_i . The output beam is symbolized by $\overrightarrow{k_{out}}$, but it is not involved in the present calculation.

First, the total resulting reflectivity is calculated for a general case with an ideal degree of polarisation (DOP), i.e., a purely linear polarisation, and the first derivative vs. the refractive index is estimated. It is made of a p-pol and a s-pol components as shown by Eqs (A-13) and (A-14) in Appendix A:

$$\begin{split} R_{tot} &= \left(\frac{\cos\theta \; \sin\phi_i}{\sin\phi_i'} \; \big| r_p \big| \right)^2 + \left(\frac{\sin\theta}{\sin\phi_i'} \; \big| r_s \big| \right)^2 \\ &\qquad \qquad (1.a) \\ R_{frac} &= \frac{R_{tot}(n_{sub} + 0.01) - R_{tot}(n_{sub} - 0.01)}{R_{tot}(n_{sub}).0.02} \end{split}$$

However, to be more specific, it makes sense to include the DOP, so these equations become as calculated in Appendix B:

$$R_{tot-DOP} = \left[\left(\frac{\cos\theta \sin\phi_i}{\sin\phi_i'} \left| r_p \right| \right)^2 + \left(\frac{\sin\theta}{\sin\phi_i'} \left| r_s \right| \right)^2 \right] \left(\frac{DOP}{\sqrt{DOP^2 + 1}} \right)^2 + \left[\left(\frac{\cos\theta \sin\phi_i}{\sin\phi_i'} \left| r_s \right| \right)^2 + \left(\frac{\sin\theta}{\sin\phi_i'} \left| r_p \right| \right)^2 \right] \left(\frac{1}{\sqrt{DOP^2 + 1}} \right)^2$$

$$(2.a)$$

$$R_{frac-DOP} = \frac{R_{tot-DOP}(n_{sub} + 0.01) - R_{tot-DOP}(n_{sub} - 0.01)}{R_{tot-DOP}(n_{sub}).0.02}$$
(2.b

The details of the calculation are shown in appendices A and B at the end of this document.

Both are plotted as contour plots in Fig. 4, vs the 2 angles: the horizontal angle ϕ_i and the tilt angle θ of the partially reflective surface. Somehow, $R_{frac-DOP}$ is arbitrary. Indeed, only the zero-line is relevant since it is the target.

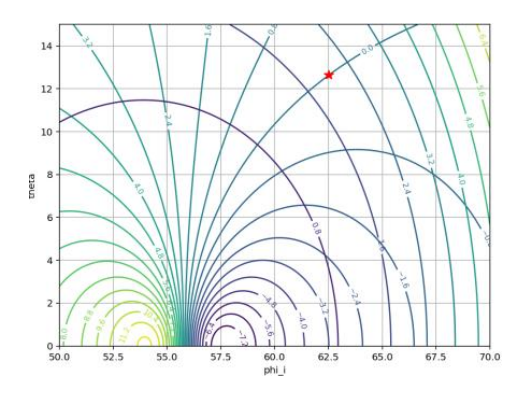


Fig. 4: Contour plots of $R_{frac-DOP}$ and $R_{tot-DOP}$, calculated from Eqs (2). The specific point of the zero-line at a reflectivity of 2 % is also calculated. The DOP is 20. The red asterisk corresponds to the angles of 62.5° and 12.6°.

A specific point (red asterisk) has been calculated, set on the zero-line ($R_{frac-DOP} = 0$) and corresponding to $R_{tot-DOP} = 2\%$, for a DOP = 20, which corresponds to a power ratio of 400, which is relatively common.

It is also possible to calculate the polarization angle α_p vs. the same 2 angles. α_p has been calculated in Appendix A, for a horizontal input polarisation:

$$\alpha_p = \tan^{-1} \frac{\sin \theta}{\cos \theta \sin \phi_i}$$
 (3)

It is related to a purely linear polarisation, i.e., an infinite value of DOP. If DOP was finite, the polarisation angle would be the angle of the major axis.

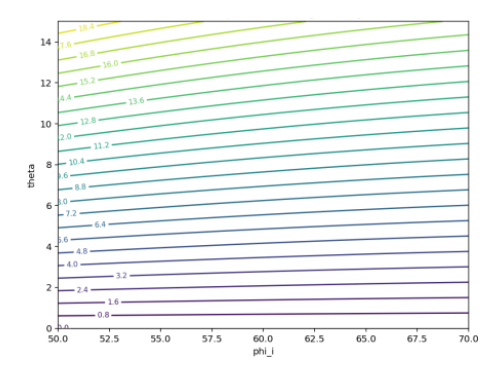


Fig. 5: Contour plot of the polarisation angle, for a horizontal (oriented along y) input polarisation.

The polarisation angle is shown in Fig. 5. As expected, it is close to the tilt angle θ , albeit not the same.

Once we have identified where should sit the point of interest (red asterisk in Fig.4) It would be interesting to investigate this specific point, in particular how the total reflectivity varies around this point. Indeed, one can wonder whether it corresponds to a minimum or not, like the Brewster's angle. It could be done by looking at the reflectivity vs the horizontal angle ϕ_i , for a given tilt angle δ . This done in Fig. 5.

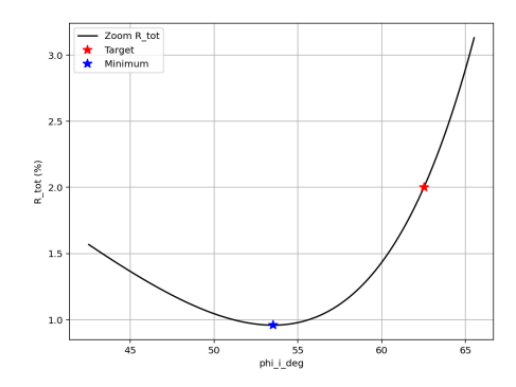


Fig. 5: Total reflectivity zoomed around the points of interest, i.e., the target point in red asterisk, and the minimum in blue asterisk. In this particular case, $n_{sub} = 1.47$, DOP = 20, $\theta = 12.6^{\circ}$, and the target reflectivity on the zero-line is 2 %. It is shown with the red asterisk. In practice, the easiest to see is the minimum reflectivity, which is shown on the graph with the blue asterisk. The difference in ϕ_i between the 2 asterisks is here 9°.

In Fig. 5, one can see that the difference in ϕ_i between the target point and the minimum reflectivity is 9°. This could be a strategy for reaching the target point accurately.

In practice, there might still be a power drift due to miscalibration. To refine the adjustment, the sign of miscalibration should tell on which side of the zero-line the system is.

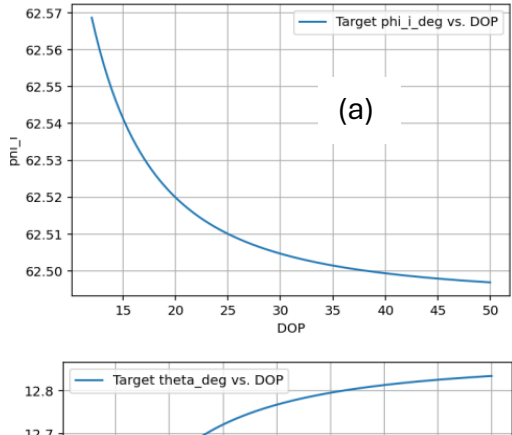
Further considerations

The system includes a feedback mechanism that utilizes the reflected fraction to control the laser beam's power. By measuring the power of the reflected portion, the system can adjust the laser's output to maintain a stable power level, even under varying environmental conditions. This feedback control is essential for applications requiring precise and stable laser beam properties.

In practice, the effect shown in this paper is seen with the sign of miscalibration. Indeed, the adjustment of the reflective pick-off can be optimized. From Fig. 4. one can see that for a given tilt angle, adjusting the horizontal angle can bring the system on one side of the zero-line or the other, which make the derivative positive or negative. Consequently, in practice, it will make the miscalibration 'positive' or 'negative'. Therefore, observing the behaviour of the laser tells in which direction the horizontal angle should be changed to reach the vicinity of the zero-line.

The effect of DOP can also be investigated, as it can change substantially the optimal configuration. It also justifies the need of the empirical approach explained above.

Lasers are often polarized linearly, especially those with intracavity doubling. The power ratio (Ratio between major axis over minor axis) can even be around 1600, which makes a DOP (as defined in Eqs (B-1)) of 40. However, because of residual stress birefringence, it can be sometimes as low as 12. In Fig. 6, the target angles (defining how the pick-off plate should be oriented) are plotted vs. DOP from 12 to 50. n_{sub} and n_0 are still taken as 1.47 and 1, respectively.



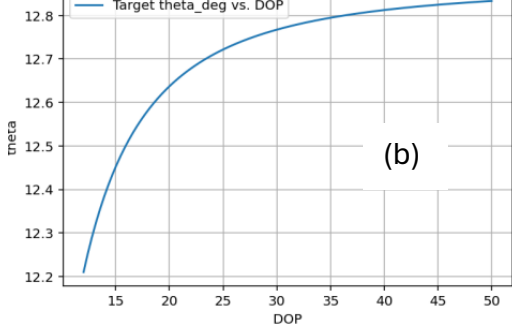


Fig. 6: Target angles [(a): ϕ_i and (b): θ] for $n_{sub} = 1.47$ and $n_0 = 1$. They have been calculated for $R_{frac-DOP} = 0$ and $R_{tot-DOP} = 2\%$.

From Fig. 6, it can be noticed that for the lowest values of DOP (left side of the curve), ϕ_i tends to increase, and θ tends to decrease substantially.

Conclusion

This white paper presents an advanced laser system that achieves stable reflection properties under varying environmental conditions. By using the vertically tilted Brewster pick-off technique and optimizing the polarization angle, the system ensures that the reflected fraction of the laser beam remains invariant to changes in temperature or contamination. This innovation enhances optical performance, extends component longevity, and offers significant benefits for applications requiring precise control and measurement of laser beam properties, paving the way for more reliable and accurate laser-based technologies.

This white paper provides a comprehensive overview of the advanced laser system, its theoretical foundation, and practical implications. It serves as a valuable resource for understanding the innovation and its potential impact on various applications. Moreover, the thorough calculation allows to accurately predicts the behaviour of actual systems.

Appendix A

The purpose of this appendix is to perform the thorough calculation of the formulas involved. This calculation is performed according to the scheme in Fig. 3.

We will need to build the formulas of R_{tot} , the total (p-pol + s-pol) reflectivity on the surface of interest, and its first derivative vs. the refractive index of the surface, relatively to R_{tot} . We will call it R_{frac} . These formulas will need to be depending on the angles in Fig. 3.

First, the normal input beam is defined as:

$$\overrightarrow{k_{in}} = \begin{pmatrix} 0\\0\\1 \end{pmatrix} \tag{A-1}$$

Where the referential is defined as (x,y,z) in Fig. 3.

The reflective surface is defined by the normal vector:

$$\vec{n} = \begin{pmatrix} \sin \theta \\ -\cos \theta \sin \phi_i \\ -\cos \theta \cos \phi_i \end{pmatrix}$$
 (A-2)

Where θ is the tilt angle of the reflective surface, and ϕ_i is the horizontal angle of the beam vs. the reflective surface.

One can set:

$$\vec{n} \cdot \left(-\overrightarrow{k_{in}} \right) = \cos \phi_i'$$
 (A-3)

Where ϕ_i is the angle of incidence (AOI). Combining (A-1), (A-2), and (A-3) leads to:

$$\cos \phi_i' = \cos \theta \cos \phi_i \qquad (A-4)$$

This can give the angle of incidence (AOI) ϕ_i '.

It should be also possible to calculate the p-pol and s-pol components. This is necessary to calculate the total reflectivity, by using the Fresnel's equations.

First, the p-pol component is in the plane of polarization, and the s-pol is perpendicular to it, i.e., perpendicular to both $\overrightarrow{k_m}$ and \overrightarrow{n} .

The latter is easy to calculate, by using the cross product. We can introduce \vec{m} , the unitary vector defining the s-pol. One can write:

$$\vec{m} = \frac{\vec{k}_{in} \times \vec{n}}{\|\vec{k}_{in} \times \vec{n}\|} \tag{A-5}$$

Which can also be written:

$$\vec{m} = \frac{1}{\sin \phi_i} \begin{pmatrix} \cos \theta \sin \phi_i \\ \sin \theta \\ 0 \end{pmatrix}$$
(A-6)

This is where we can introduce δ , the angle of the s-pol with the x-direction:

$$\vec{m} = \begin{pmatrix} \cos \delta \\ \sin \delta \\ 0 \end{pmatrix} \qquad (A-7)$$

It is worthwhile to notice that δ is also the angle between the p-pol direction and the polarisation (on y), as shown in Fig. A-1:

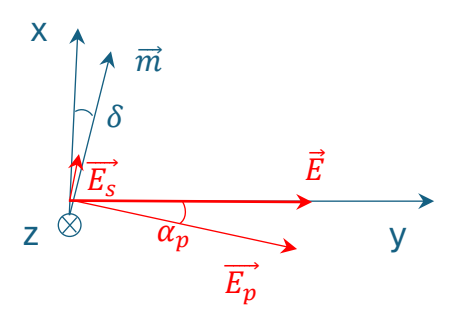


Fig. A-1: Description of the vectors involved, perpendicularly to z-axis

Since the incident polarisation is along y, the input polarisation can be defined as:

$$\vec{E} = \begin{pmatrix} 0 \\ 1 \\ 0 \end{pmatrix} \tag{A-8}$$

From this one can introduce the polarisation angle α_p , which is the angle between the p-pol component and the y-direction, because:

$$\vec{E} = \overrightarrow{E_s} + \overrightarrow{E_n} \tag{A-9}$$

One can then deduce:

$$\cos \alpha_p = \frac{\cos \theta \sin \phi_i}{\sin \phi_i'}$$
 (A-10.a)

$$\sin \alpha_p = \frac{\sin \theta}{\sin \phi_i'} \tag{A-10.b}$$

The polarisation angle can then be extracted from:

$$\tan \alpha_p = \frac{\sin \theta}{\cos \theta \sin \phi_i}$$
 (A-11)

This is useful to calculate the total reflectivity, by adding the p-pol and s-pol reflectivities. The sign of $\tan \alpha_p$ depends on how the polarisation is defined, since α_p is always modulo π . We might need to consider $|\tan \alpha_p|$, i.e., $|\alpha_p|$. Anyway, it will be used with squares on sines and cosines.

However, the goal is to separate the p-pol and s-pol components. In the present case, the major component is p-pol, with the smallest reflectivity, and the minor one is s-pol, with the biggest reflectivity. As a result, the total reflectivity is:

$$R_{tot} = \left(\cos \alpha_p \ |r_p|\right)^2 + \left(\sin \alpha_p \ |r_s|\right)^2 \tag{A-12}$$

Where r_p and r_s are the amplitude reflectivities for pand s-polarisations, respectively. It can then be explicated as:

$$R_{tot} = \left(\frac{\cos\theta \sin\phi_i}{\sin\phi_i'} \left| r_p \right| \right)^2 + \left(\frac{\sin\theta}{\sin\phi_i'} \left| r_s \right| \right)^2$$
(A-13)

It looks like a complicated function to plot, but it is not difficult to do. We will use Python, which has some built-in functions for that.

One can then define the relative derivative of R_{tot} vs. n_{sub} , the refractive index of the substrate. This is what we want to set to 0. It can be defined as follows:

$$R_{frac} = \frac{R_{tot}(n_{sub} + 0.01) - R_{tot}(n_{sub} - 0.01)}{R_{tot}(n_{sub}) \cdot 0.02}$$
(A.14)

It is not calculated analytically, but rather numerically, which is easier in a Python code.

Appendix B

The purpose of this appendix is to modify the previous calculation to adapt it to the general case of a nonpurely linear polarisation, which is the most general and common case.

First, the degree of polarisation needs to be defined. It corresponds to the ratio of amplitudes between the two components E_{major} and E_{minor} , in the case of slight depolarisation or elliptical polarisation. These two components can then be written:

$$E_{minor} = \frac{1}{\sqrt{DOP^2 + 1}}$$
 (B-1.a)

$$E_{major} = \frac{DOP}{\sqrt{DOP^2 + 1}}$$
 (B-1.b)

In order $DOP = \frac{E_{major}}{E_{minor}}$ and $E_{minor}^2 + E_{major}^2 = 1$. From Fig. A-1, the total reflectivity can then be rewritten:

$$R_{tot-DOP} = (\cos \alpha_p)^2 (E_{major})^2 |r_p|^2 + (\sin \alpha_p)^2 (E_{minor})^2 |r_p|^2 + (\sin \alpha_p)^2 (E_{minor})^2 |r_s|^2 + (\cos \alpha_p)^2 (E_{minor})^2 |r_s|^2$$
(B-2)

Where r_p and r_s are the reflectivities in amplitude of the p- and s-polarisations, respectively.

$$\begin{split} R_{tot-DOP} &= \left[\left(\frac{\cos\theta \; \sin\phi_i}{\sin\phi_i'} \; |r_p| \right)^2 \right. \\ &\quad + \left(\frac{\sin\theta}{\sin\phi_i'} \; |r_s| \right)^2 \right] \left(\frac{DOP}{\sqrt{DOP^2 + 1}} \right)^2 \\ &\quad + \left[\left(\frac{\cos\theta \; \sin\phi_i}{\sin\phi_i'} \; |r_s| \right)^2 \right. \\ &\quad + \left. \left(\frac{\sin\theta}{\sin\phi_i'} \; |r_p| \right)^2 \right] \left(\frac{1}{\sqrt{DOP^2 + 1}} \right)^2 \end{split} \tag{B-3}$$

In a similar manner as before, the derivative function can be defined as:

$$\begin{split} R_{frac-DOP} &= \\ \frac{R_{tot-DOP}(n_{sub}+0.01) - R_{tot-DOP}(n_{sub}-0.01)}{R_{tot-DOP}(n_{sub}).0.02} \end{split}$$
 (B-4)

References

- [1] Cox, A., & Cotteverte, J.-C. (2015). *Laser* system (U.S. Patent No. US 2016033775 A1). United States Patent and Trademark Office.
- [2] Born, Max; Wolf, Emil (1999). Principles of optics: electromagnetic theory of propagation, interference and diffraction of light (7th expanded ed.). Cambridge: Cambridge University Press.